Articles in PresS. Am J Physiol Lung Cell Mol Physiol (July 22, 2016). doi:10.1152/ajplung.00124.2016

Cigarette smoke causes acute airways disease and exacerbates chronic obstructive lung disease in neonatal mice

Jie Jia[1]*, Thomas M. Conlon[1]*, Carolina Ballester Lopez[1], Michael Seimetz[2], Mariola Bednorz[2], Zhe Zhou-Suckow[3], Norbert Weissmann[2], Oliver Eickelberg[1,4], Marcus A. Mall[3#], Ali Önder Yildirim[1#]

1. Comprehensive Pneumology Center (CPC), Institute of Lung Biology and Disease, Helmholtz Zentrum München, Munich, Germany, Member of the German Center for Lung Research (DZL)

2. Excellence Cluster Cardio-Pulmonary System (ECCPS), Justus-Liebig-University Giessen, Department of Internal Medicine, Universities of Giessen and Marburg Lung Center (UGMLC), D-35392 Giessen, Germany, Member of the German Center for Lung Research (DZL)

3. Department of Translational Pulmonology, Translational Lung Research Center Heidelberg (TLRC), University of Heidelberg, Heidelberg, Germany, Member of the German Center for Lung Research (DZL)

4. University Hospital of the Ludwig Maximilians University (LMU), Munich, Germany

* Contributed equally to the work

# Contributed equally as senior authors

Author Contributions: JJ, OE, MAM & AÖY designed experiments; JJ, CLB, MS, MB & TMC conducted experiments; JJ, TMC, MAM & AÖY wrote the manuscript; all authors contributed to scientific discussions and approved the manuscript.

Running Head: CS-induced neonatal airways disease

Address for Correspondance:

Ali Önder Yildirim

Comprehensive Pneumology Center

Institute of Lung Biology and Disease

Helmholtz Zentrum München

Ingolstädter Landstraße 1

85764 Neuherberg

Germany

oender.yildirim@helmholtz-muenchen.de

Tel. +49 89 3187-4037

Fax. +49 89 3187-2400

Abstract

Epidemiological evidence demonstrates a strong link between postnatal cigarette smoke (CS)-exposure and increased respiratory morbidity in young children. However, how CS induces early onset airways disease in young children and how it interacts with endogenous risk factors remains poorly understood. We, therefore exposed 10 day old neonatal wild-type and βENaC-transgenic mice with cystic fibrosis like lung disease to CS for 4 days. Neonatal wild-type mice exposed to CS demonstrated increased numbers of macrophages and neutrophils in the BALF which was accompanied by increased levels of *Mmp12* and *Cxcl1*. BALF from βENaC-transgenic mice contained greater numbers of macrophages which did not increase following acute CS-exposure, however there was significant increase in airway neutrophilia compared to filtered air transgenic and CS-exposed wild-type controls. Interestingly, wild-type and βENaC-transgenic mice demonstrated epithelial airway and vascular remodeling following CS-exposure. Morphometric analysis of lung sections revealed that CS-exposure caused increased mucus accumulation in the airway lumen of neonatal βENaC-transgenic mice compared to wild-type controls, which was accompanied by an increase in the number of goblet cells and *Muc5ac* upregulation. We conclude that short-term CS exposure i) induces acute airways disease with airway epithelial and vascular remodeling in neonatal wild-type mice; and ii) exacerbates airway inflammation, mucus hypersecretion and mucus plugging in neonatal βENaC-transgenic mice with chronic lung disease. Our results in neonatal mice suggest that young children may be highly susceptible to develop airways disease in response to tobacco smoke exposure and that adverse effects may be aggravated in children with underlying chronic lung diseases.

Key words: airways disease, newborn, cigarette smoke, inflammation, mucus

Introduction

Chronic airways diseases including recurrent wheezing, chronic bronchitis and asthma constitute a major cause of morbidity in young children and evidence from epidemiologic studies identified tobacco smoke exposure as an important risk factor for the development of chronic airways disease in early childhood (9, 29, 37). However, current knowledge on the *in vivo* pathogenesis of airways disease induced by environmental tobacco smoke in young children, and how tobacco smoke exposure interacts with endogenous risk factors and underlying chronic lung disease remains poorly understood.

In adult smokers, chronic tobacco smoke exposure is a key risk factor of chronic bronchitis associated with influx of macrophages and neutrophils into the airways, goblet cell metaplasia and mucus hypersecretion and structural lung damage (14, 16, 20, 31, 32), and these pathologies are at least in part recapitulated by chronic cigarette smoke (CS) exposure in adult mice (3, 5, 13, 18, 36). In comparison, studies on the effect of CS in children, or short-term CS exposure in neonatal mice more closely reflecting environmental exposure in young children remain limited. In children who died of sudden infant death syndrome, it was found that maternal smoking is associated with airway wall thickening (8) and a study of newborn mice exposed to two weeks of CS straight after birth reported an increase in the presence of alveolar macrophages, albeit to a lesser extent than in adult mice (27). However, the consequences of short-term CS exposure with regard to airway inflammation, mucus hypersecretion and tissue remodeling in neonates *in vivo,* remains to be fully elucidated.

The aim of this study was, therefore, to determine the *in vivo* effects of acute CS exposure on airway inflammation and lung morphology in neonatal wild-type mice as a model of parental CS exposure of heathy infants. Second, we used the βENaC-transgenic mouse as an established model of cystic fibrosis (CF) lung disease to assess the impact of CS exposure in the context of chronic underlying lung disease.

These mice over express the β-subunit of the epithelial sodium ion channel (βENaC), a key protein in regulating airway surface liquid (26), along with chloride ion channels (33), under the control of the club cell secretary protein promoter, causing enhanced airway Na^+ absorption which results in airway surface dehydration and reduced mucus clearance. The mice develop spontaneous early onset lung disease that shares key features with CF in children including airway mucus plugging, chronic airway inflammation and structural lung damage (23, 25). Specifically, we hypothesized i) that neonatal wild-type mice are susceptible to develop airways disease even after short-term CS exposure; and ii) that adverse effects of CS are enhanced in βENaC-transgenic mice with obstructive lung disease. To test these hypotheses, we exposed neonatal wild-type and βENaC-transgenic mice to CS for 4 days and compared indices of airway inflammation, epithelial, vascular and alveolar remodeling and airway mucus obstruction after this short-term CS exposure. Using this *in vivo* model of postnatal CS exposure, we demonstrate that tobacco smoke produces acute airways disease in neonatal mice and that adverse effects are enhanced in concurrent chronic obstructive lung disease. These results provide novel insights into the link between tobacco smoke exposure and increased respiratory morbidity early in life and are consistent with its adverse effects on lung health in young children.

Materials and Methods

Experimental animals

βENaC-transgenic mice on a C57BL/6 background (17, 23), were bred in-house with C57BL/6NCrl mice (Charles River Laboratories, Sulzfeld, Germany). Mice were housed under specific pathogen free conditions at a constant temperature and humidity with a 12-hour light cycle and allowed food and water *ad libitum*. All animal experiments were performed according to strict governmental and international guidelines and were approved by the local government for the administrative region of Upper Bavaria.

Cigarette smoke exposure

10 day old βENaC-transgenic mice and their wild-type littermate controls (males and females) were whole body exposed to 100% mainstream CS at 500 mg/m^3 total particulate matter generated from 3R4F Research Cigarettes (filter removed, Tobacco Research Institute, University of Kentucky, Lexington, KY), for 50 min twice per day for 4 days. Pups were separated from their mothers during the smoking period. In brief, to mimic natural human smoking habits, CS was generated with 2 seconds of puff and 4 seconds of break by a membrane pump and drawn into the exposure chamber (19). FA- exposed animals were used as controls. Mice were sacrificed the day after final smoking exposure (age 15 days), following the assessment of lung function, by terminal exsanguination of the anaesthetized mice.

Lung function measurement

Mice were anaesthetized with ketamine and xylazine, tracheostomized and their pulmonary function analysed using the flexiVent system (Scireq, Montreal, Canada). A mean lung volume similar to that of spontaneous breathing mice was obtained by ventilating with a tidal volume of 10ml/kg at a frequency of 150 breaths/min. Lung mechanical properties were tested using the SnapShot perturbation. Four readings per mice were taken and meaned.

Bronchoalveolar lavage fluid (BALF) differential cell counting

Lungs were lavaged with 3x500 µl of sterile PBS (Gibco, Life Technologies, Darmstadt, Germany). Cells were pelleted at 400g and resuspended in RPMI-1640 medium (Gibco, Life Technologies, Darmstadt, Germany) for the total cell count using a haemocytometer. Cytospins of the cell suspension were then prepared and stained using May-Grünwald-Giemsa for differential cell counting (200 cells/sample) using morphological criteria.

Lung tissue processing

Right lungs were snap frozen in liquid nitrogen, homogenized and total RNA isolated (peqGOLD Total RNA Kit, Peqlab, Erlangen, Germany) for gene expression analysis. The left lungs were fixed at a constant pressure (20 cm fluid column) by instilling intratracheally PBS buffered 6% paraformaldehyde, and then embedded into paraffin for immunohistochemistry and histological analysis with Hematoxylin and Eosin (H&E) and Periodic Acid-Schiff (PAS) staining. For studies of airway mucus, mouse lungs were immersion fixed without prior BAL. For PAS staining, lung sections were taken at the level of the proximal intra-pulmonary main axial airway near the hilus with a thickness of 3 µm, as described previously (25).

Quantitative real time RT-PCR

Mouse cDNA was synthesized using Random Hexamers and Reverse Transcriptase (Applied Biosystems, Darmstadt, Germany) from right lung isolated total RNA. Mouse *Muc5ac* (Forward 5'-ATCGAGAGGAGCGTTGACAC-3', Reverse 5'-ATGCAGCCTTGCTTGAGG-3'), *Muc5b* (Forward 5'-AGAAACTGGAGCTGGGCTCT-3', Reverse 5'-TGACTGTCTCCGGTGAGTTCT-3'), *Cxcl1* (Forward 5`-CCGAAGTCATAGCCACAC-3', Reverse 5`- GTGCCATCAGAGCAGTCT-3') and *Mmp12* (Forward 5`-TGTACCCCACCTACAGATACCTTA-3', Reverse 5`-CCATAGAGGGACTGAATGTTACGT-3') gene expression levels were analysed using Platinum SYBR Green qPCR SuperMix (Applied Biosystems) on a StepOnePlus 96 well Real-Time-PCR system (Applied Biosystems, Carlsbad, CA), and calculated relative to the housekeeping gene *Hprt1* (Forward 5`-AGCTACTGTAATGATCAGTCAACG-3', Reverse 5`-AGAGGTCCTTTTCACCAGCA-3'). Relative expression is defined as $2^{-\Delta Ct}$ where $\Delta Ct = Ct_{target} - Ct_{housekeeping}$.

Immunohistochemistry

Deparaffinized and rehydrated lung sections were blocked for endogenous peroxidase activity with 1.8% (v/v) H_2O_2 solution (Sigma-Aldrich, St. Louis, MO). Epitope retrieval was undertaken using heated HIER citrate buffer (pH 6.0, ZYTOMED Systems GmbH, Berlin, Germany) in a decloaking chamber (Biocare Medical, Concord, CA). Sections were then blocked using Rodent Blocking Buffer (Biocare Medical), before being incubated at 4°C overnight with primary antibodies against Mmp12 (1:200, ab66157, Abcam, Cambridge, UK), Gr1 (1:50, ab2557, Abcam) or Galectin-3 (1:100, sc-20157, Santa Cruz Biotechnology Inc., Dallas, Texas). This was followed by a 1hr incubation at room temperature with an alkaline phosphatase-labeled secondary antibody (Biocare Medical) and then signal amplification with

158 the chromogen substrate Vulcan fast red (Biocare Medical). Sections were counterstained with
159 hematoxylin (Sigma-Aldrich), dehydrated in xylene and mounted with Entellan (Merck Millipore,
160 Billerica, MA).

161

162 *Quantitative morphometry*

163 Stained tissue sections were analysed with design-based stereology using an Olympus BX51 light
164 microscope equipped with the new Computer Assisted Stereological Toolbox (newCAST, Visiopharm,
165 Hoersholm, Denmark) as described previously (18, 28). Lung airspace enlargement was analysed by
166 quantifying the mean linear intercept (MLI) of the H&E stained lung sections. Briefly, 30 random fields of
167 view per lung were superimposed with points and a line grid. The points hitting air space (P_{air}) and
168 intercepts of lines with alveolar septa (I_{septa}) were counted to calculate the MLI, using $MLI = \sum P_{air} \times L(p) /$
169 $\sum I_{septa} \times 0.5$, where L(p) is the line length per point.

170 For quantitative assessment of airway mucus accumulation, the PAS-stained lung sections were
171 analysed using a volume counting toolbox across 100 random fields of view per lung. The volume of
172 airway mucus (V_{mucus}) was calculated as the number of points hitting on positively stained
173 mucosubstances (P_{mucus}) normalised to the number of line intercepts with airway basement membrane
174 (I_{airway}), using the formula $V_{mucus} = \sum P_{mucus} \times 0.5 \times L(p) / \sum I_{airway}$.

175 To calculate the percentage of goblet cells a frame grid was superimposed on lung section images across
176 100 fields of view per lung. The percentage of points hitting on PAS positively stained airway epithelial
177 cells compared to the points hitting on all airway epithelial cells were calculated.

The thickness of the airway epithelium was calculated as the number of points hitting epithelial cells ($P_{epithelium}$) normalised to the number of line intercepts with airway basement membrane (I_{airway}), using the formula $V_{epithelium} = \sum P_{epithelium} \times 0.5 / \sum I_{airway}$.

Muscularization of pulmonary arterial vessels

The muscularization of pulmonary arterial vessels was determined as previously described (34) from lung paraffin sections. The sections were stained with a 1:900 diluted α-smooth muscle actin antibody (clone 1A4, Sigma-Aldrich, Munich, Germany) to visualize the muscle layer and a 1:900 dilution of the anti-human von Willebrand-factor antibody to allow identification of vessels (Dako, Hamburg, Germany). The degree of muscularization of small vessels (20–70 µm) was microscopically determined by vascular morphometry using the Qwin software (Leica, Wetzlar, Germany) and expressed as averaged % of the vessel circumference being α-smooth muscle actin positive. 85 vessels were analysed from each lung lobe in a randomized and blinded fashion.

Statistical analysis

Data were analysed with GraphPad Prism 6 software (GraphPad software, La Jolla, CA) and presented as mean values ± s.e.m.. Groups of n = 12-16 mice were exposed to CS or FA, with the specific numbers used for each analysis given in the appropriate figure legend. Statistical analyses were performed using a two-tailed unpaired *t*-test or one-way ANOVA following Bonferroni post testing as indicated. $P < 0.05$ was taken to indicate statistical significance.

Results

CS exposure causes acute airway inflammation in neonatal wild-type mice and exacerbates inflammation in βENaC-transgenic mice

To determine if acute CS exposure causes airway inflammation we measured the number of inflammatory cells in the BALF of neonatal (15 day old) wild-type and βENaC-transgenic mice after 4 days of exposure to CS or filtered air (FA). There was a clear increase in the total cell count in BALF of wild-type mice following acute CS exposure (Fig. 1A) which was predominantly due to an increase in macrophage and neutrophil numbers (Fig. 1B, C). βENaC-transgenic mice had a higher inflammatory total cell count in the BALF compared to wild-type controls after exposure to FA (Fig. 1A). This was largely composed of macrophages (Fig. 1B), with a trend towards increased neutrophils compared to FA wild-type controls (Fig. 1C), but this did not reach statistical significance. Following acute exposure to CS there was no change in the number of macrophages present in the BALF of βENaC-transgenic mice and this was similar to the number observed in CS-exposed wild-type mice (Fig. 1B). There was however, a strong increase in the number of neutrophils detected in the BALF of βENaC-transgenic mice following CS exposure, which was significantly increased compared to CS-exposed wild-type mice (Fig. 1C).

For further characterization of the inflammation triggered by acute CS exposure, we undertook immunohistochemistry using anti-Galectin-3 antibody for macrophages and anti-Gr1 antibody for neutrophils on lung sections from mice that had not undergone the BALF procedure. Fig. 1D clearly shows that there is an increase in the number of septal tissue macrophages present in the lungs of wild-type mice following exposure to CS. Furthermore, more macrophages are detectable in the lungs of βENaC-transgenic mice exposed to FA than their wild-type counter parts, and that these do not significantly increase in number following exposure to CS (Fig. 1D). Fig. 1E demonstrates that no

neutrophils are detectable in the lungs of wild-type mice exposed to FA, but a very small number can be seen associated with the airway following acute CS exposure. FA-exposed βENaC-transgenic mice showed Gr1 positive cells mainly in the airway lumen that increased in number following acute CS exposure (Fig. 1E).

Next, we determined transcript levels of the neutrophil chemoattractant *Cxcl1* (KC) and *Mmp12* as a marker of activated macrophages. Wild-type mice exposed to acute CS exhibited higher mRNA levels for *Cxcl1* (KC) and *Mmp12* in total lung homogenate compared to FA controls (Fig. 2A, B). Concomitant with the increased airway neutrophil number observed in βENaC-transgenic mice (Fig. 1D), FA-exposed βENaC-transgenic mice demonstrated higher mRNA levels for *Cxcl1* than their wild-type counterparts (Fig. 2A), which increased further following CS exposure. *Mmp12* mRNA levels were also greater in the lungs of FA-exposed βENaC-transgenic mice compared to wild-type FA controls (Fig. 2B), which increased further following CS exposure and was significantly greater than that exhibited in wild-type CS-exposed mice (Fig. 2B). The changes in *Mmp12* gene expression were also confirmed at the protein level by immunohistochemistry on lung tissue sections. Fig. 2C demonstrates that airway epithelial cells were positively stained for Mmp12 in wild-type animals only following acute CS, whereas positively stained airway epithelial cells could also be detected in the FA-exposed βENaC-transgenic mice, which was further enhanced upon CS exposure. Mmp12 positive macrophages, surprisingly, could not be detected in the lungs of wild-type mice even after CS exposure, whereas a large number of Mmp12 positively stained macrophages could be observed in the lungs of the βENaC-transgenic mice following acute CS exposure, with a large number accumulating in the airways (Fig. 2C). Interestingly, albeit to a lesser extent, Mmp12 positively stained macrophages could also be detected in the airways of FA-exposed βENaC-transgenic mice (Fig. 2C). Taken together, this data supports that short-term CS induces

243 a robust inflammatory response in neonatal mice that is exacerbated in predisposed βENaC-transgenic
244 mice.

245

246 **Acute CS exposure causes remodeling of the airway epithelium and pulmonary vessels**

247 We next investigated whether acute CS exposure had effects on the morphology of the airway
248 epithelium and pulmonary vasculature. Exposure of neonatal (10 day old) wild-type mice to 4 days of CS
249 increased the thickness of the airway epithelium compared to FA controls (Fig. 3A). This was confirmed
250 by analysis of morphological quantification using the newCAST system (Fig. 3B). The airway epithelium
251 of neonatal βENaC-transgenic mice after exposure to FA did not differ to that of wild-type FA controls
252 (Fig. 3A, B). After exposure to CS the βENaC-transgenic mice also appeared to have thicker airway
253 epithelium compared to FA-exposed controls (Fig. 3A), but this did not reach statistical significance (Fig.
254 3B).

255 In addition to acute effects on the airway epithelium, we found that short term CS exposure of neonatal
256 wild-type mice had a significant effect on pulmonary vessels. Specifically, we observed a pronounced
257 increase in the muscularization of small pulmonary vessels (20-70 μm in diameter) compared to FA
258 controls (Fig. 4A, B). Similar to their wild-type counterparts, βENaC-transgenic mice exposed only to FA,
259 demonstrated a low level of small vessel muscularization, which increased significantly following
260 exposure to acute CS (Fig. 4A, B). There was no difference in the level of small vessel muscularization
261 between the wild-type and βENaC-transgenic mice following CS exposure (Fig. 4B). These results
262 demonstrate that even a short CS exposure in neonatal mice is sufficient to trigger remodeling of the
263 airway epithelium and pulmonary vessels.

264

Airspace size and lung function was not altered by acute CS exposure

We next investigated effects of short-term CS exposure on lung function and distal airspace morphology. As shown in Fig. 5 acute exposure to CS had no effect on alveolar morphology (Fig. 5A), mean linear intercept (Fig. 5B) or lung function parameters including dynamic compliance, elastance or resistance of the lung (Fig. 5C-E). As expected from previous studies (25, 42) FA-exposed βENaC-transgenic mice showed emphysema-like distal airspace enlargement (Fig. 5A), which was confirmed by quantitative morphometry (MLI of 24.60 ± 1.92 µm in βENaC-transgenic vs 15.55 ± 0.94 µm in wild-type, $P<0.01$, Fig. 5B). There was however no further enlargement of the airspaces following acute CS exposure in the βENaC-transgenic mice (Fig. 5A, B). In line with this we did not detect changes in the level of cell death, however a slight reduction in cell proliferation was observed following exposure of either wild-type or βENaC-transgenic mice to CS in lung sections stained by immunohistochemistry for cleaved (active)-caspase 3 and Ki67, respectively (data not show). Consistent with the spontaneous emphysema observed in the FA-exposed βENaC-transgenic mice, these animals also displayed impaired lung function with increased dynamic compliance and reduced total lung resistance compared to the wild-type controls (Fig. 5C-E). Exposure of the βENaC-transgenic mice to acute CS for 4 days did not alter the lung function further (Fig. 5C-E) indicating that despite remodeling of airway and pulmonary vessels the spontaneous emphysema of the βENaC-transgenic mice is not aggravated by acute CS exposure.

Acute CS exposure induces goblet cell metaplasia and increased mucin expression in βENaC-transgenic mice

Finally, we studied effects of acute CS exposure on goblet cell numbers, mucin expression and intraluminal mucus content in neonatal wild-type and βENaC-transgenic mice. Consistent with previous

studies (25), PAS staining of lung sections revealed mucus accumulation in the airways of 15 day old βENaC-transgenic mice that was not detectable in wild-type controls (Fig. 6A). Acute CS exposure, did not induce mucus accumulation in the airways of wild-type mice, but significantly increased the density and volume of the accumulated mucus in βENaC-transgenic mice compared to CS-exposed wild type animals, as determined by morphometric analysis using the newCAST system (Fig. 6B). In addition, we observed metaplasia of airway goblet cells in the βENaC-transgenic but not in wild-type mice post CS exposure (Fig. 6C and D). This was quantified (Fig. 6D) as the percentage of PAS positive airway epithelial cells, with the CS exposed βENaC-transgenic mice demonstrating 43.12 ± 2.98% goblet cells compared to 6.74 ± 2.51% (P<0.001) in wild-type mice exposed to CS and 18.77 ± 6.32% (P<0.01) goblet cells in βENaC-transgenic mice exposed to FA. Similar, *Muc5ac* and *Muc5b* gene expression in total lung homogenate were only increased in the βENaC-transgenic mice exposed to CS (Fig. 6E). Taken together this data suggests that acute CS exposure triggers increased mucus production in βENaC-transgenic mice.

Discussion

In this study, we have established a new mouse model of postnatal CS exposure and CS-induced exacerbation of CF-like chronic obstructive lung disease in neonatal mice. We demonstrate that exposure of neonatal (10 day old) wild-type mice to 4 days of acute CS resulted in a macrophage and neutrophil predominant inflammation of the airways. Further, we show for the first time in young mice that the inflammation triggered by such a short exposure period to CS, is accompanied by airway epithelial thickening and pulmonary vessel remodeling. Then using neonatal βENaC-transgenic mice as an established model of CF-like lung disease featuring spontaneous mucus hypersecretion, airway mucus plugging and inflammation in the first week of life, we demonstrate that short-term CS exacerbated the chronic bronchitis phenotype in this model. These results are consistent with the clinical observation and epidemiologic data suggesting that environmental tobacco smoke exposure is a major risk factor for the development of airways disease in children (9, 29, 37).

It is widely appreciated that exposure of adult mice to acute CS results in a strong inflammatory response driven by macrophages and neutrophils (6, 11, 19). A study of newborn mice exposed to two weeks of CS straight after birth also reported an increase in the presence of alveolar macrophages (27). Here we confirmed (Fig. 1, 2) that acute CS-exposed neonatal wild-type mice also demonstrate a strong increase in BALF macrophage numbers, which was accompanied by increased *Mmp12* mRNA expression in total lung homogenates and positively stained airway epithelial cells in immunohistochemically stained sections. Aside from Mmp12 production by alveolar macrophages following short-term exposure to CS in mice (7), CS extract has been shown to upregulate MMP12 in human airway-like epithelial cells (21). Interestingly, the βENaC-transgenic mice exposed only to FA have increased macrophage numbers in the BALF compared to wild-type controls, accompanied by higher levels of total lung *Mmp12* gene expression and Mmp12 positive airway macrophages and epithelial cells (Fig. 1, 2). These data confirm

that impaired mucociliary clearance and mucus stasis triggered by airway surface dehydration in βENaC-transgenic mice, already triggers a strong inflammatory response at neonatal ages (40). This response is then enhanced following short-term exposure to CS, suggesting that young children with CF or other underlying chronic obstructive lung disease may require little CS exposure to exacerbate their condition.

A significant finding from our study is that in both wild-type and βENaC-transgenic mice we observe that an acute exposure to CS at neonatal ages results in thickening of the airway epithelium (Fig. 3). It has been previously reported that exposure of Swiss albino mice or H mice from birth for 120 days to CS resulted in pronounced hyperplasia of the bronchial epithelium (1, 2), but these are tumor prone mice exposed chronically. Meanwhile, exposure to CS for 10 days across a two week period in adult Balb/c mice induced airway epithelial hyperplasia and mucous cell metaplasia that was inhibited by blockade of DP2, a prostaglandin D_2 receptor (38). Of note, CS-induced airway epithelial thickening occurred to a similar extent in both wild-type and βENaC-transgenic mice suggesting that direct effects of CS rather than chronic inflammation is the driving force behind airway epithelial cell hyperplasia. Given the relatively small diameter of airways in infants, this mucosal thickening may contribute to airflow obstruction and recurrent wheezing in young children exposed to CS.

We also demonstrate that exposure to acute CS in newborn mice results in pronounced increases in muscularization of the small pulmonary vessels (20-70 μm in diameter), in both wild-type and βENaC-transgenic mice (Fig. 4). It has been previously shown in adult rats that short-term exposure to CS induced pulmonary vascular remodeling (45), but most studies have focused on the effect of chronic CS exposure (34, 43, 44). Pulmonary vascular remodeling is prevalent amongst patients with CS-induced COPD (30) and has been shown to contribute to emphysema development in chronic CS-exposed mice (34). Acute CS exposure does not lead to emphysema development, however βENaC-transgenic mice spontaneously develop emphysema-like changes, but we show that this is independent of pulmonary

vascular remodeling. Nevertheless, that short-term CS exposure can lead to pulmonary vascular remodeling in the newborn should be carefully considered as a potential contributing factor to respiratory disease and pulmonary hypertension later in life.

A strength with our model is the accumulation of mucus in the airways of βENaC-transgenic mice (Fig. 6). The pathophysiology of chronic bronchitis in patients and the associated increase in airway infections, is closely related to intraluminal obstruction of the airways caused by mucus adhesion, mucus plaques and in severe cases mucus plugging (4, 24). A weakness with existing models of CS exposure in mice is that wild-type mice exposed to CS, even chronically out to 6 months, do not demonstrate evidence of mucus accumulation (12, 18). This is confirmed here in neonatal wild-type mice, despite a strong inflammatory response and airway epithelial remodeling following acute CS exposure, we see no evidence of goblet cell metaplasia or changes to *Muc5ac* or *Muc5b* gene expression, major secreted mucins (39). Interestingly, in the neonatal βENaC-transgenic mice with underlying chronic obstructive airways disease, acute CS smoke exposure resulted in goblet cell metaplasia and increased expression of *Muc5ac* and *Muc5b*. We speculate that reduced mucociliary clearance in βENaC-transgenic mice may cause impaired clearance of CS, which may lead to the more severe neutrophilia producing higher levels of neutrophil elastase acting as a potent stimulus of goblet cell metaplasia in the airways (10, 41). Interestingly, in a recent study Seys et al. (35) exposed adult βENaC-transgenic mice to CS for up to 8 weeks. They confirmed that adult βENaC-transgenic mice have increased goblet cells and mucus production compared to wild-type controls, but unlike our observation with newborn mice, adult βENaC-transgenic mice did not exhibit goblet cell metaplasia after CS exposure. The likely reason for this is the inherent difference in the number of goblet cells in the airways between young and adult mice (22). Taken together this data suggests that young children with CF and other chronic airways diseases may be more susceptible to CS exposure.

βENaC-transgenic mice also demonstrate emphysema-like structural lung damage (10, 25, 40), which we confirmed by lung function analysis and quantification of MLI on H&E stained lung sections to be present in our 15 day old transgenic mice (Fig. 5). Interestingly, crossing the βENaC-transgenic mice onto a neutrophil elastase or Mmp12 deficient background reduced inflammation and emphysema in these mice (10, 40). Despite an increase in inflammation and Mmp12 upregulation in the lungs of βENaC-transgenic mice following exposure to acute CS, we do not see any deterioration in lung function or airspace enlargement. This is not surprising as we have previously shown that in wild-type mice we require 4 months of CS exposure to induce emphysematous changes to the lungs (18). However, the CS-exposed βENaC-transgenic mice demonstrated both increased mucus production and epithelial thickening of the airways expected to cause increased airway resistance and airflow limitation due to airway obstruction. We speculate that increased airway resistance was not detected in our lung function measurements, because the FlexiVent uses a one compartment model integrating the resistances of the conducting airways and distal airspaces in the lung parenchyma, where the reduction in resistance caused by the emphysema present in the βENaC-transgenic mice most likely overrides any changes due to airway obstruction. One would hypothesize that emphysema progression would be accelerated in the βENaC-transgenic mice following a longer exposure to CS, and that we only assessed acute CS exposure is a limitation of this current study. Although we saw no changes to airspace enlargement following acute exposure to CS in the neonatal mice, it is important to again highlight that we did observe airway remodeling occurring in these young animals after CS exposure (Fig. 3). Hogg et al. (15) proposes that emphysema development stems from an initial lesion in the small airways, we should therefore consider that these early pathological changes may sow the seed for chronic obstructive lung disease later in life. Interestingly, in the study by McGrath-Morrow et al. (27), they following up mice at 8 weeks of age that received two weeks of CS from birth, and reported reduced alveolar number and an increase in MLI size compared to 8 week old mice that did not receive the CS exposure at birth.

In summary, we established a novel neonatal murine model to assess *in vivo* effects of postnatal CS exposure in wild-type and βENaC-transgenic mice with CF-like obstructive lung disease. In this model, we demonstrate for the first time that short-term CS exposure is sufficient to induce acute airways disease characterized by neutrophilic airway inflammation, mucosal thickening and vascular remodeling in neonatal wild-type mice. Further, we show that CS exacerbates airway inflammation and mucus hypersecretion in neonatal βENaC-transgenic mice with chronic CF-like lung disease. These results provide novel insights into the link between CS exposure and increased respiratory morbidity during early life and demonstrate that even short-term CS exposure has substantial adverse effects on lung health and exacerbates underlying chronic lung disease such as CF *in vivo*. We expect that this novel model will be useful for studies of therapeutic intervention, as well as further elucidation of the factors that determine resolution versus chronicity of CS-induced respiratory pathology and thus define the development of disease phenotypes such as recurrent wheezing, chronic bronchitis and asthma that are more common in infants and young children who are exposed to parental tobacco smoke.

Acknowledgements

The authors acknowledge the technical assistance of Christine Hollauer and Lisa Fröhlich.

Grants

This work was supported in part by the Helmholtz Association and The German Center for Lung Research (DZL).

Disclosures

MAM is listed on a patent application filed by the University of North Carolina, describing the βENaC-overexpressing mouse (patent number: 7514593; filing date: May 2003). Of note, the βENaC-overexpressing mouse has been deposited at the Jackson Laboratory.

References

1. **Balansky R, Ganchev G, Iltcheva M, Nikolov M, Steele VE, and De Flora S**. Differential carcinogenicity of cigarette smoke in mice exposed either transplacentally, early in life or in adulthood. *International journal of cancer Journal international du cancer* 130: 1001-1010, 2012.
2. **Balansky R, Ganchev G, Iltcheva M, Steele VE, D'Agostini F, and De Flora S**. Potent carcinogenicity of cigarette smoke in mice exposed early in life. *Carcinogenesis* 28: 2236-2243, 2007.
3. **Churg A, Cosio M, and Wright JL**. Mechanisms of cigarette smoke-induced COPD: insights from animal models. *American journal of physiology Lung cellular and molecular physiology* 294: L612-631, 2008.
4. **Collawn JF, and Matalon S**. CFTR and lung homeostasis. *American journal of physiology Lung cellular and molecular physiology* 307: L917-923, 2014.
5. **D'Hulst A I, Maes T, Bracke KR, Demedts IK, Tournoy KG, Joos GF, and Brusselle GG**. Cigarette smoke-induced pulmonary emphysema in scid-mice. Is the acquired immune system required? *Respiratory research* 6: 147, 2005.
6. **D'Hulst A I, Vermaelen KY, Brusselle GG, Joos GF, and Pauwels RA**. Time course of cigarette smoke-induced pulmonary inflammation in mice. *The European respiratory journal* 26: 204-213, 2005.
7. **da Hora K, Valenca SS, and Porto LC**. Immunohistochemical study of tumor necrosis factor-alpha, matrix metalloproteinase-12, and tissue inhibitor of metalloproteinase-2 on alveolar macrophages of BALB/c mice exposed to short-term cigarette smoke. *Experimental lung research* 31: 759-770, 2005.
8. **Elliot J, Vullermin P, and Robinson P**. Maternal cigarette smoking is associated with increased inner airway wall thickness in children who die from sudden infant death syndrome. *American journal of respiratory and critical care medicine* 158: 802-806, 1998.
9. **Galobardes B, Granell R, Sterne J, Hughes R, Mejia-Lancheros C, Davey Smith G, and Henderson J**. Childhood wheezing, asthma, allergy, atopy, and lung function: different socioeconomic patterns for different phenotypes. *American journal of epidemiology* 182: 763-774, 2015.
10. **Gehrig S, Duerr J, Weitnauer M, Wagner CJ, Graeber SY, Schatterny J, Hirtz S, Belaaouaj A, Dalpke AH, Schultz C, and Mall MA**. Lack of neutrophil elastase reduces inflammation, mucus hypersecretion, and emphysema, but not mucus obstruction, in mice with cystic fibrosis-like lung disease. *American journal of respiratory and critical care medicine* 189: 1082-1092, 2014.
11. **Givi ME, Akbari P, Boon L, Puzovic VS, Bezemer GF, Ricciardolo FL, Folkerts G, Redegeld FA, and Mortaz E**. Dendritic cells inversely regulate airway inflammation in cigarette smoke-exposed mice. *American journal of physiology Lung cellular and molecular physiology* 310: L95-102, 2016.
12. **Guerassimov A, Hoshino Y, Takubo Y, Turcotte A, Yamamoto M, Ghezzo H, Triantafillopoulos A, Whittaker K, Hoidal JR, and Cosio MG**. The development of emphysema in cigarette smoke-exposed mice is strain dependent. *American journal of respiratory and critical care medicine* 170: 974-980, 2004.
13. **Hautamaki RD, Kobayashi DK, Senior RM, and Shapiro SD**. Requirement for macrophage elastase for cigarette smoke-induced emphysema in mice. *Science* 277: 2002-2004, 1997.
14. **Hogg JC**. Pathophysiology of airflow limitation in chronic obstructive pulmonary disease. *Lancet* 364: 709-721, 2004.

15. **Hogg JC, Chu F, Utokaparch S, Woods R, Elliott WM, Buzatu L, Cherniack RM, Rogers RM, Sciurba FC, Coxson HO, and Pare PD**. The nature of small-airway obstruction in chronic obstructive pulmonary disease. *The New England journal of medicine* 350: 2645-2653, 2004.
16. **Innes AL, Woodruff PG, Ferrando RE, Donnelly S, Dolganov GM, Lazarus SC, and Fahy JV**. Epithelial mucin stores are increased in the large airways of smokers with airflow obstruction. *Chest* 130: 1102-1108, 2006.
17. **Johannesson B, Hirtz S, Schatterny J, Schultz C, and Mall MA**. CFTR regulates early pathogenesis of chronic obstructive lung disease in betaENaC-overexpressing mice. *PloS one* 7: e44059, 2012.
18. **John-Schuster G, Hager K, Conlon TM, Irmler M, Beckers J, Eickelberg O, and Yildirim AO**. Cigarette smoke-induced iBALT mediates macrophage activation in a B cell-dependent manner in COPD. *American journal of physiology Lung cellular and molecular physiology* 307: L692-706, 2014.
19. **John G, Kohse K, Orasche J, Reda A, Schnelle-Kreis J, Zimmermann R, Schmid O, Eickelberg O, and Yildirim AO**. The composition of cigarette smoke determines inflammatory cell recruitment to the lung in COPD mouse models. *Clinical science* 126: 207-221, 2014.
20. **Lacoste JY, Bousquet J, Chanez P, Van Vyve T, Simony-Lafontaine J, Lequeu N, Vic P, Enander I, Godard P, and Michel FB**. Eosinophilic and neutrophilic inflammation in asthma, chronic bronchitis, and chronic obstructive pulmonary disease. *The Journal of allergy and clinical immunology* 92: 537-548, 1993.
21. **Lavigne MC, and Eppihimer MJ**. Cigarette smoke condensate induces MMP-12 gene expression in airway-like epithelia. *Biochemical and biophysical research communications* 330: 194-203, 2005.
22. **Livraghi A, Grubb BR, Hudson EJ, Wilkinson KJ, Sheehan JK, Mall MA, O'Neal WK, Boucher RC, and Randell SH**. Airway and lung pathology due to mucosal surface dehydration in {beta}-epithelial Na+ channel-overexpressing mice: role of TNF-{alpha} and IL-4R{alpha} signaling, influence of neonatal development, and limited efficacy of glucocorticoid treatment. *Journal of immunology* 182: 4357-4367, 2009.
23. **Mall M, Grubb BR, Harkema JR, O'Neal WK, and Boucher RC**. Increased airway epithelial Na+ absorption produces cystic fibrosis-like lung disease in mice. *Nature medicine* 10: 487-493, 2004.
24. **Mall MA**. Unplugging Mucus in Cystic Fibrosis and Chronic Obstructive Pulmonary Disease. *Annals of the American Thoracic Society* 13 Suppl 2: S177-185, 2016.
25. **Mall MA, Harkema JR, Trojanek JB, Treis D, Livraghi A, Schubert S, Zhou Z, Kreda SM, Tilley SL, Hudson EJ, O'Neal WK, and Boucher RC**. Development of chronic bronchitis and emphysema in beta-epithelial Na+ channel-overexpressing mice. *American journal of respiratory and critical care medicine* 177: 730-742, 2008.
26. **Matalon S, Bartoszewski R, and Collawn JF**. Role of epithelial sodium channels in the regulation of lung fluid homeostasis. *American journal of physiology Lung cellular and molecular physiology* 309: L1229-1238, 2015.
27. **McGrath-Morrow S, Rangasamy T, Cho C, Sussan T, Neptune E, Wise R, Tuder RM, and Biswal S**. Impaired lung homeostasis in neonatal mice exposed to cigarette smoke. *American journal of respiratory cell and molecular biology* 38: 393-400, 2008.
28. **Muhlfeld C, Hegermann J, Wrede C, and Ochs M**. A review of recent developments and applications of morphometry/stereology in lung research. *American journal of physiology Lung cellular and molecular physiology* 309: L526-536, 2015.
29. **Pattenden S, Antova T, Neuberger M, Nikiforov B, De Sario M, Grize L, Heinrich J, Hruba F, Janssen N, Luttmann-Gibson H, Privalova L, Rudnai P, Splichalova A, Zlotkowska R, and Fletcher T**. Parental smoking and children's respiratory health: independent effects of prenatal and postnatal exposure. *Tobacco control* 15: 294-301, 2006.

30. **Peinado VI, Pizarro S, and Barbera JA**. Pulmonary vascular involvement in COPD. *Chest* 134: 808-814, 2008.
31. **Saetta M, Di Stefano A, Maestrelli P, Ferraresso A, Drigo R, Potena A, Ciaccia A, and Fabbri LM**. Activated T-lymphocytes and macrophages in bronchial mucosa of subjects with chronic bronchitis. *The American review of respiratory disease* 147: 301-306, 1993.
32. **Saetta M, Turato G, Baraldo S, Zanin A, Braccioni F, Mapp CE, Maestrelli P, Cavallesco G, Papi A, and Fabbri LM**. Goblet cell hyperplasia and epithelial inflammation in peripheral airways of smokers with both symptoms of chronic bronchitis and chronic airflow limitation. *American journal of respiratory and critical care medicine* 161: 1016-1021, 2000.
33. **Salomon JJ, Spahn S, Wang X, Fullekrug J, Bertrand CA, and Mall MA**. Generation and functional characterization of epithelial cells with stable expression of SLC26A9 Cl- channels. *American journal of physiology Lung cellular and molecular physiology* 310: L593-602, 2016.
34. **Seimetz M, Parajuli N, Pichl A, Veit F, Kwapiszewska G, Weisel FC, Milger K, Egemnazarov B, Turowska A, Fuchs B, Nikam S, Roth M, Sydykov A, Medebach T, Klepetko W, Jaksch P, Dumitrascu R, Garn H, Voswinckel R, Kostin S, Seeger W, Schermuly RT, Grimminger F, Ghofrani HA, and Weissmann N**. Inducible NOS inhibition reverses tobacco-smoke-induced emphysema and pulmonary hypertension in mice. *Cell* 147: 293-305, 2011.
35. **Seys LJ, Verhamme FM, Dupont LL, Desauter E, Duerr J, Seyhan Agircan A, Conickx G, Joos GF, Brusselle GG, Mall MA, and Bracke KR**. Airway Surface Dehydration Aggravates Cigarette Smoke-Induced Hallmarks of COPD in Mice. *PloS one* 10: e0129897, 2015.
36. **Shapiro SD, Goldstein NM, Houghton AM, Kobayashi DK, Kelley D, and Belaaouaj A**. Neutrophil elastase contributes to cigarette smoke-induced emphysema in mice. *The American journal of pathology* 163: 2329-2335, 2003.
37. **Snodgrass AM, Tan PT, Soh SE, Goh A, Shek LP, van Bever HP, Gluckman PD, Godfrey KM, Chong YS, Saw SM, Kwek K, Teoh OH, and Group GS**. Tobacco smoke exposure and respiratory morbidity in young children. *Tobacco control* 2015.
38. **Stebbins KJ, Broadhead AR, Baccei CS, Scott JM, Truong YP, Coate H, Stock NS, Santini AM, Fagan P, Prodanovich P, Bain G, Stearns BA, King CD, Hutchinson JH, Prasit P, Evans JF, and Lorrain DS**. Pharmacological blockade of the DP2 receptor inhibits cigarette smoke-induced inflammation, mucus cell metaplasia, and epithelial hyperplasia in the mouse lung. *The Journal of pharmacology and experimental therapeutics* 332: 764-775, 2010.
39. **Thornton DJ, Rousseau K, and McGuckin MA**. Structure and function of the polymeric mucins in airways mucus. *Annual review of physiology* 70: 459-486, 2008.
40. **Trojanek JB, Cobos-Correa A, Diemer S, Kormann M, Schubert SC, Zhou-Suckow Z, Agrawal R, Duerr J, Wagner CJ, Schatterny J, Hirtz S, Sommerburg O, Hartl D, Schultz C, and Mall MA**. Airway mucus obstruction triggers macrophage activation and matrix metalloproteinase 12-dependent emphysema. *American journal of respiratory cell and molecular biology* 51: 709-720, 2014.
41. **Voynow JA, Fischer BM, and Zheng S**. Proteases and cystic fibrosis. *The international journal of biochemistry & cell biology* 40: 1238-1245, 2008.
42. **Wielputz MO, Eichinger M, Zhou Z, Leotta K, Hirtz S, Bartling SH, Semmler W, Kauczor HU, Puderbach M, and Mall MA**. In vivo monitoring of cystic fibrosis-like lung disease in mice by volumetric computed tomography. *The European respiratory journal* 38: 1060-1070, 2011.
43. **Wright JL, and Churg A**. Effect of long-term cigarette smoke exposure on pulmonary vascular structure and function in the guinea pig. *Experimental lung research* 17: 997-1009, 1991.
44. **Wright JL, Farmer SG, and Churg A**. A neutrophil elastase inhibitor reduces cigarette smoke-induced remodelling of lung vessels. *The European respiratory journal* 22: 77-81, 2003.

45. **Xue H, Sun K, Xie W, Hu G, Kong H, Wang Q, and Wang H**. Etanercept attenuates short-term cigarette-smoke-exposure-induced pulmonary arterial remodelling in rats by suppressing the activation of TNF-a/NF-kB signal and the activities of MMP-2 and MMP-9. *Pulmonary pharmacology & therapeutics* 25: 208-215, 2012.

Figure captions

Fig. 1

Acute CS exposure induces airway inflammation in neonatal wild-type mice and exacerbates airway neutrophilia in βENaC-transgenic mice. BALF was obtained from 15 day old βENaC-transgenic mice and wild-type littermate controls exposed to CS or FA for 4 days, and the total cell count (A), macrophage count (B) and neutrophil count (C) determined. Mean values ± s.e.m. are given. 7 mice per FA group and 11 mice per CS group from wild-type and βENaC-transgenic mice. **P* < 0.05, ***P* < 0.01, ****P* < 0.001 following a two-tailed unpaired *t*-test. (D) Representative photomicrographs of Galectin-3 and (E) Gr1 immunohistochemically stained lung sections from 5 mice per group, which had not undergone BALF collection. Positively stained cells in red: black arrow head indicates macrophages (D) and neutrophils (E). Insert is a higher power magnification of the dashed area. Scale bar: 100 μm.

Fig. 2

Acute CS exposure induces airway inflammation in neonatal wild-type mice and exacerbates constitutive inflammatory responses in βENaC-transgenic mice. The levels of *Cxcl1* (A) and *Mmp12* (B) gene expression in total lung homogenate relative to *Hprt1* was determined by qPCR (n=5 and 8 mice, for FA and CS groups respectively). Mean values ± s.e.m. are given. *P < 0.05, **P < 0.01, ***P < 0.001 following one-way ANOVA with Bonferroni post testing. $^{\#}P$ < 0.05, $^{\#\#}P$ < 0.01, $^{\#\#\#}P$ < 0.001 following a two-tailed unpaired t-test. (C) Representative photomicrographs of anti-Mmp12 immunohistochemically stained lung sections from 5 and 8 mice per FA and CS groups respectively. Positively stained cells in red. Insert is a higher power magnification of the dashed area. Scale bar: 100 μm.

Fig. 3

Acute CS exposure induces airway epithelial remodeling in neonatal wild-type and βENaC-transgenic mice. (A) Representative photomicrographs of H&E stained lung sections from 10 day old βENaC-transgenic mice and wild-type littermate controls exposed to CS or FA for 4 days. Scale bar: 50 µm. 5 and 8 mice from the FA and CS groups respectively of both mice types were assessed. (B) Epithelial thickness was quantified by design-based stereology using the newCAST system on the PAS stained lung sections depicted in Fig. 1. Mean values ± s.e.m. are given. *$P < 0.05$, following a two-tailed unpaired *t*-test.

Fig. 4

Acute CS exposure induces pulmonary vessel remodeling in neonatal wild-type and βENaC-transgenic mice. (A) Representative photomicrographs of α-smooth muscle actin and von Willebrand-factor stained lung sections from βENaC-transgenic mice and wild-type littermate controls exposed to CS or FA for 4 days. Scale bar: 50 µm. (B) The degree of small vessel (20-70 µm in diameter) muscularization in 3 mice from all groups was quantified by vascular morphometry using Leica Qwin software. Mean values ± s.e.m. are given. **P < 0.01 following one-way ANOVA with Bonferroni post testing.

Fig. 5

Acute CS exposure does not produce distal airspace enlargement in neonatal wild-type or βENaC-transgenic mice. (A) Representative photomicrographs of H&E stained lung sections from 10 day old βENaC-transgenic mice and wild-type littermate controls exposed to CS or FA for 4 days. Scale bar: 200

607 μm. (B) Airspace enlargement was quantified as the mean linear intercept by design-based stereology
608 using the newCAST system. Lung function measurements to obtain dynamic compliance (C), Elastance
609 (D) and Resistance (E) were undertaken using the flexiVent system. Data shown is the mean value ±
610 s.e.m. (n=5 and 8 mice, for FA and CS groups respectively). $^{**}P < 0.01$, $^{***}P < 0.001$, $^{****}P < 0.0001$
611 following one-way ANOVA with Bonferroni post testing. $^{\#\#}P < 0.01$ following a two-tailed unpaired t-test.

612

613 **Fig. 6**

614 **Acute CS exposure exacerbates mucus hypersecretion in neonatal βENaC-transgenic mice.** 10 day old
615 βENaC-transgenic mice and wild-type littermate controls were exposed to CS or FA for 4 days. Lung
616 sections were obtained from 3 mice per group, which had not undergone BALF collection, and stained
617 with PAS (A-D). (A) Representative photomicrographs highlighting enhanced volume and density of
618 accumulated mucus in the airways of βENaC-transgenic mice exposed to CS. Scale bar: 100 μm. (B)
619 Mucus volume was quantified by design-based stereology using the newCAST system. (C)
620 Representative photomicrographs depicting goblet cell hyperplasia in βENaC-transgenic mice following
621 exposure to CS. Scale bar: 30 μm. (D) The percentage of airway goblet cells (PAS positive) relative to
622 total airway epithelial cell number was quantified using the newCAST system. (E) The level of *Muc5ac*
623 and *Muc5b* gene expression in total lung homogenate relative to *Hprt1* was determined by qPCR (n=5
624 and 8 mice, for FA and CS groups respectively). Mean values ± s.e.m. are given. $^{*}P < 0.05$, $^{**}P < 0.01$,
625 $^{***}P < 0.001$ following one-way ANOVA with Bonferroni post testing. $^{\#}P < 0.05$ following two-tailed
626 unpaired *t*-test.

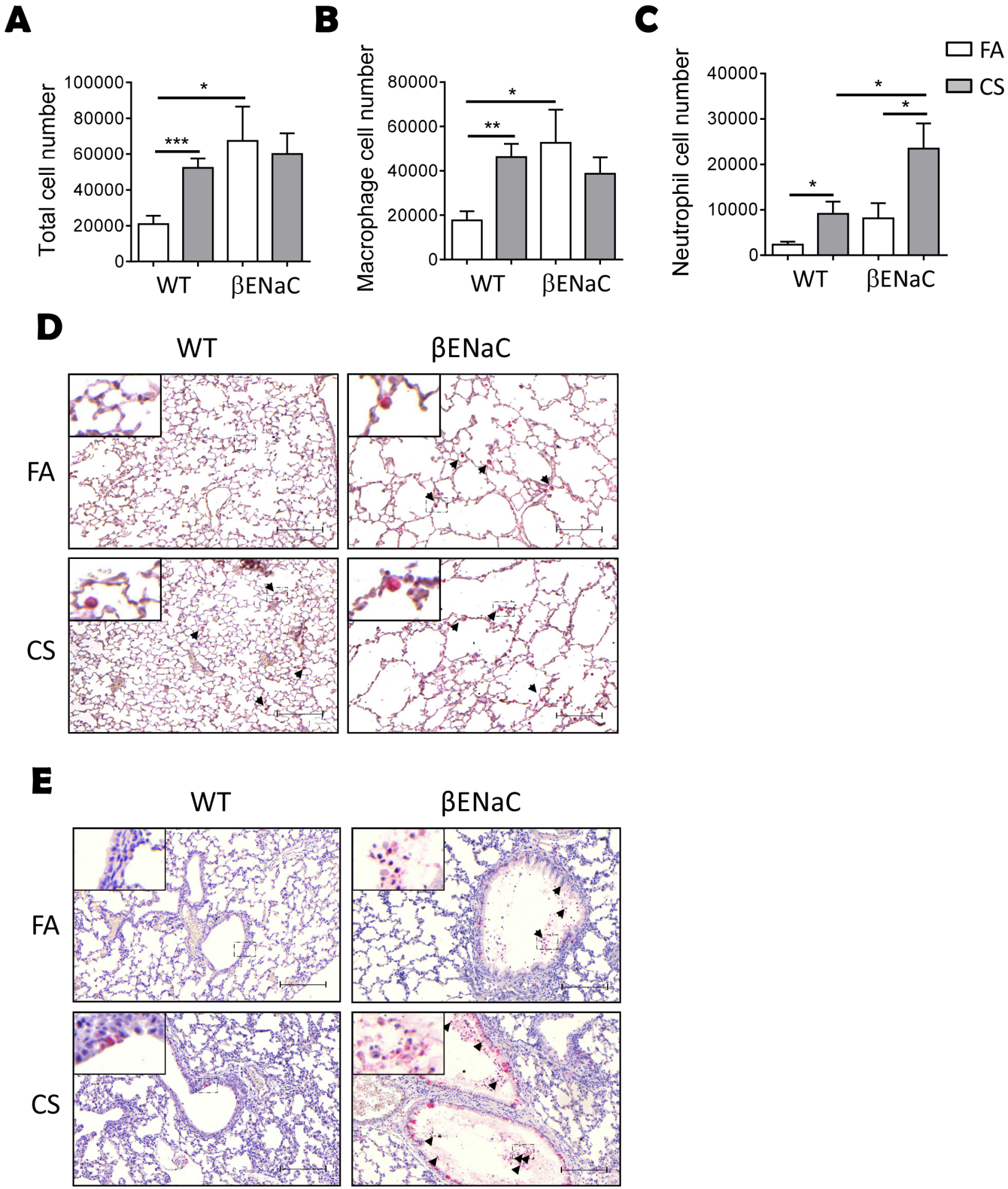
A
Total cell number
100000
80000
60000
40000
20000
0
*
***
WT
βENaC
B
Macrophage cell number
80000
60000
40000
20000
0
*
**
WT
βENaC
C
Neutrophil cell number
40000
30000
20000
10000
0
*
*
*
FA
CS
WT
βENaC
D
WT
βENaC
FA
CS
E
WT
βENaC
FA
CS

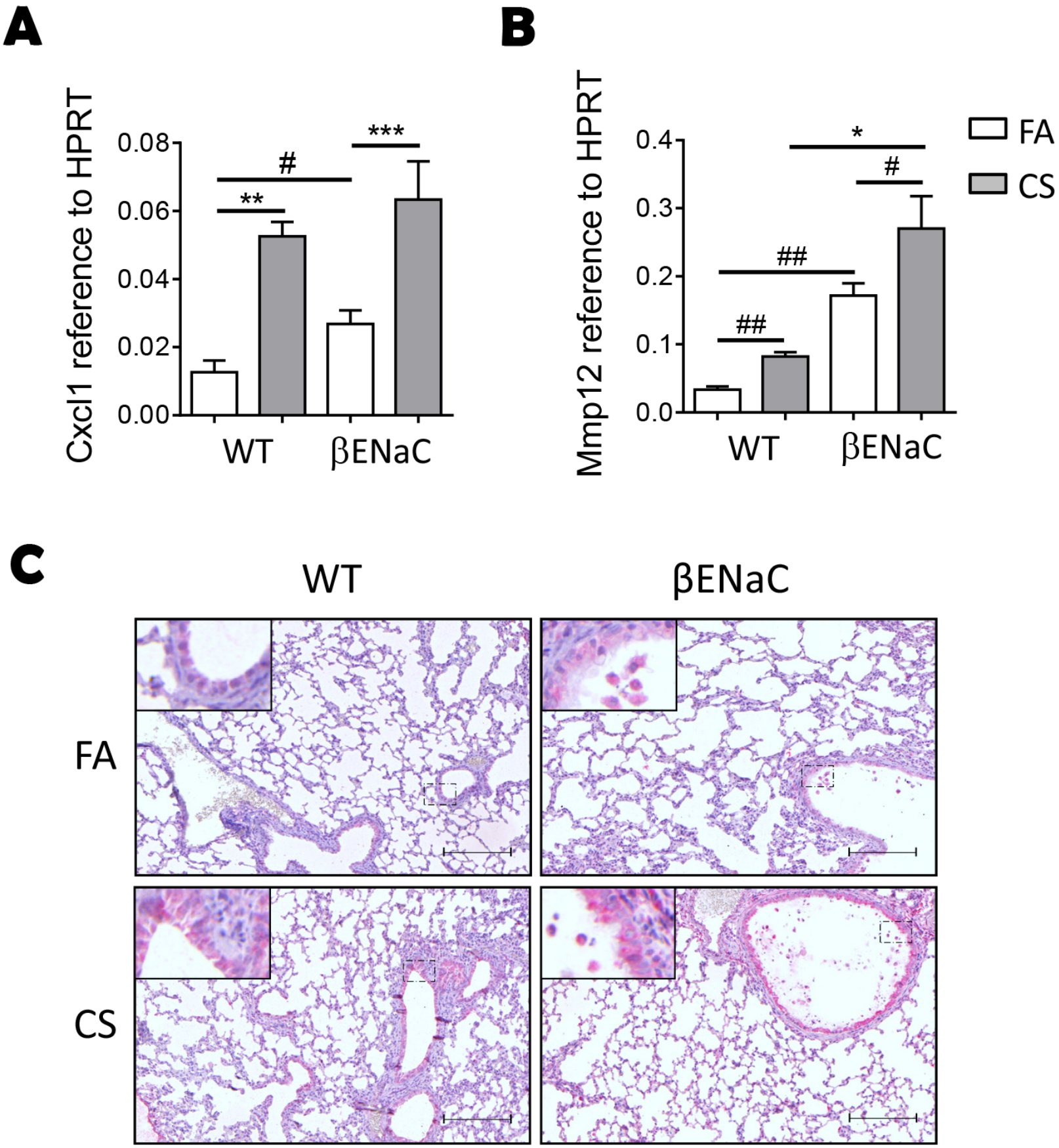
A
Cxcl1 reference to HPRT
0.08
0.06
0.04
0.02
0.00
**
#
***
WT
βENaC
B
Mmp12 reference to HPRT
0.4
0.3
0.2
0.1
0.0
*
#
##
##
WT
βENaC
FA
CS
C
WT
βENaC
FA
CS

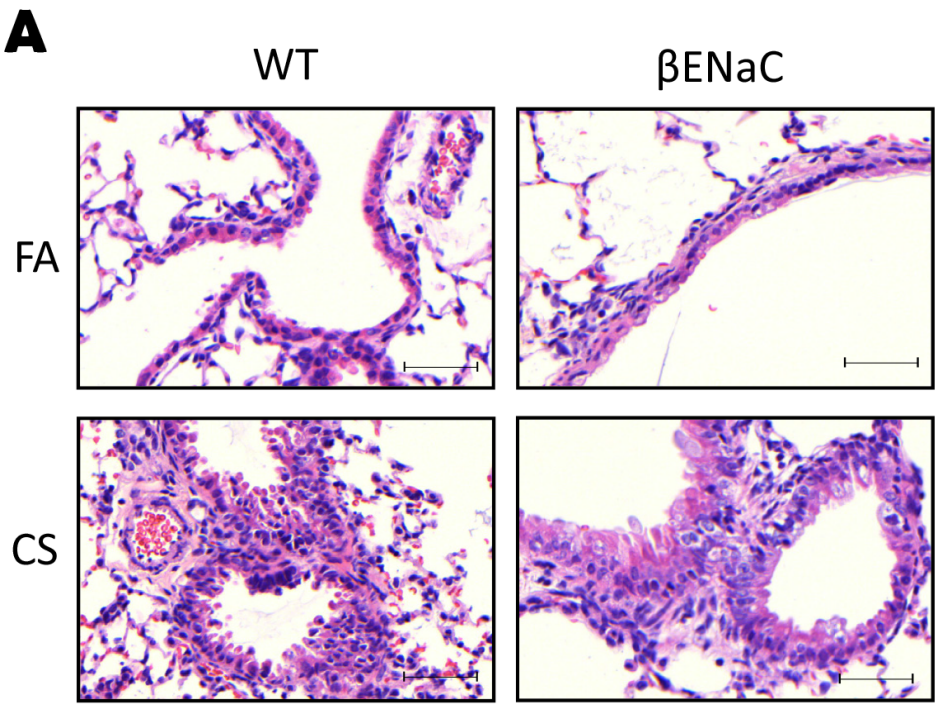
A
WT
βENaC
FA
CS

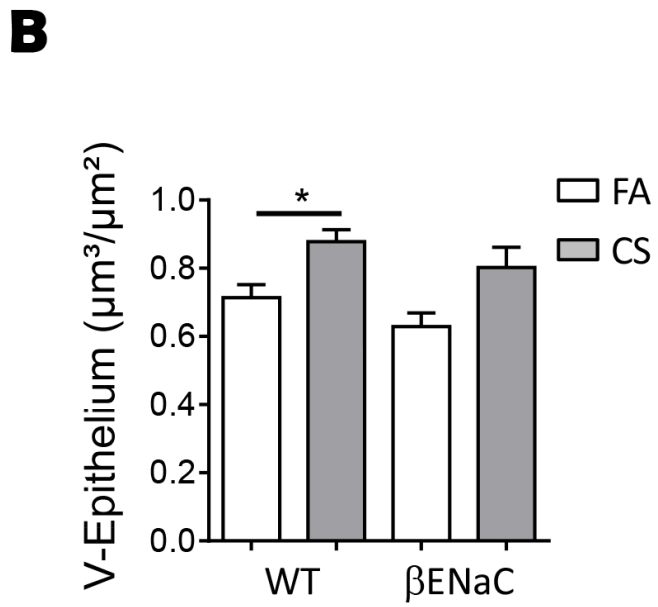
B
V-Epithelium (μm³/μm²)
1.0
0.8
0.6
0.4
0.2
0.0
*
FA
CS
WT
βENaC

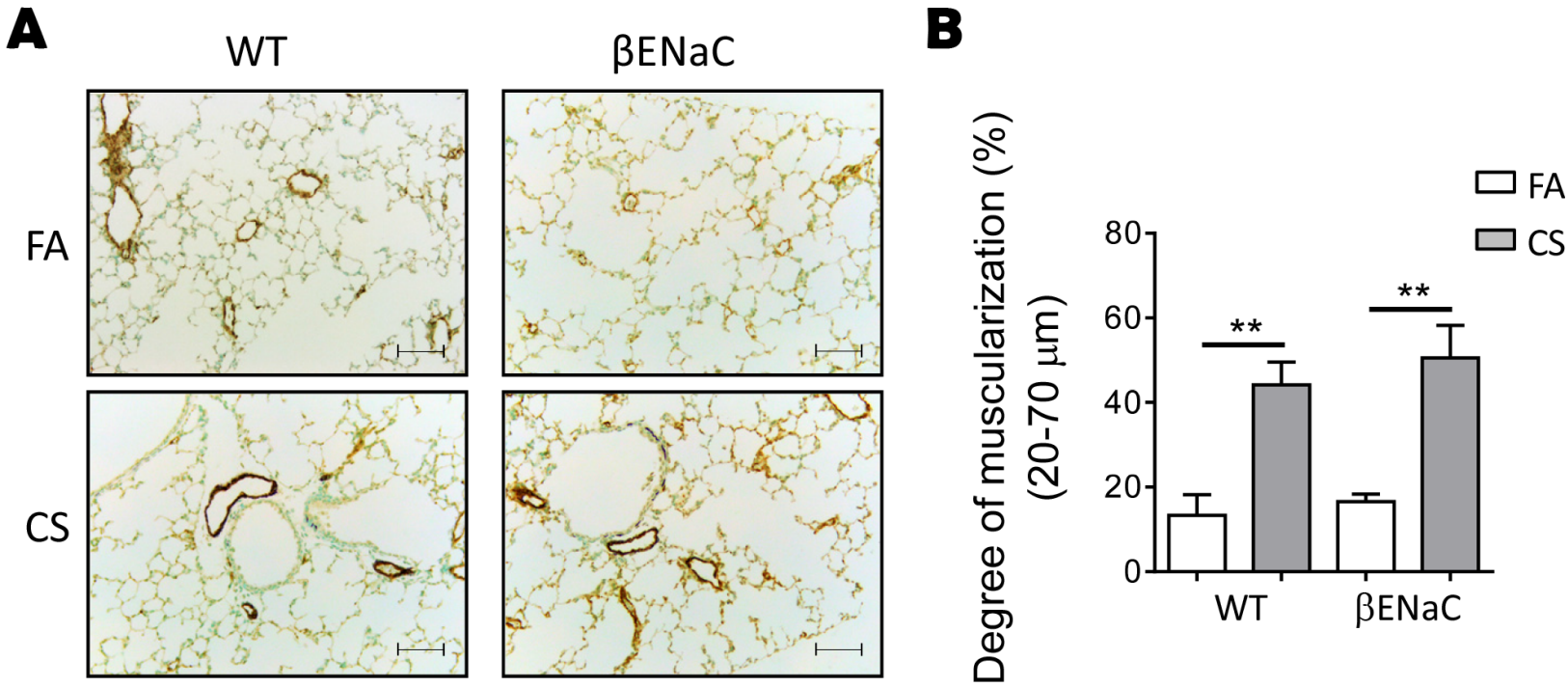
A
WT
βENaC
FA
CS
B
Degree of muscularization (%)
(20-70 μm)
FA
CS
80
60
40
20
0
**
**
WT
βENaC

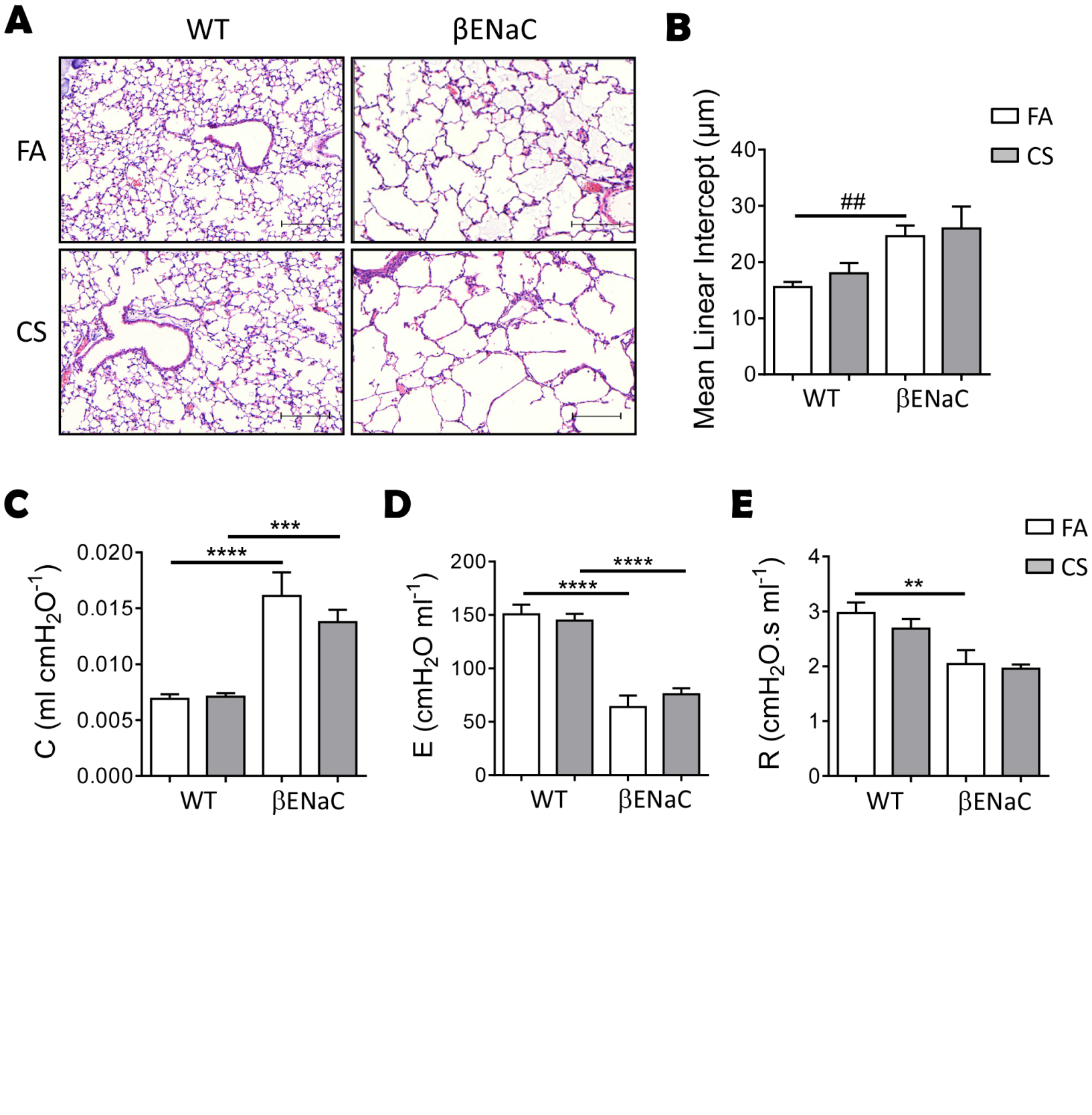
A
WT
βENaC
FA
CS
B
Mean Linear Intercept (μm)
FA
CS
##
WT
βENaC
C
C (ml cmH2O-1)
***
****
WT
βENaC
D
E (cmH2O ml-1)
****
****
WT
βENaC
E
R (cmH2O.s ml-1)
FA
CS
**
WT
βENaC

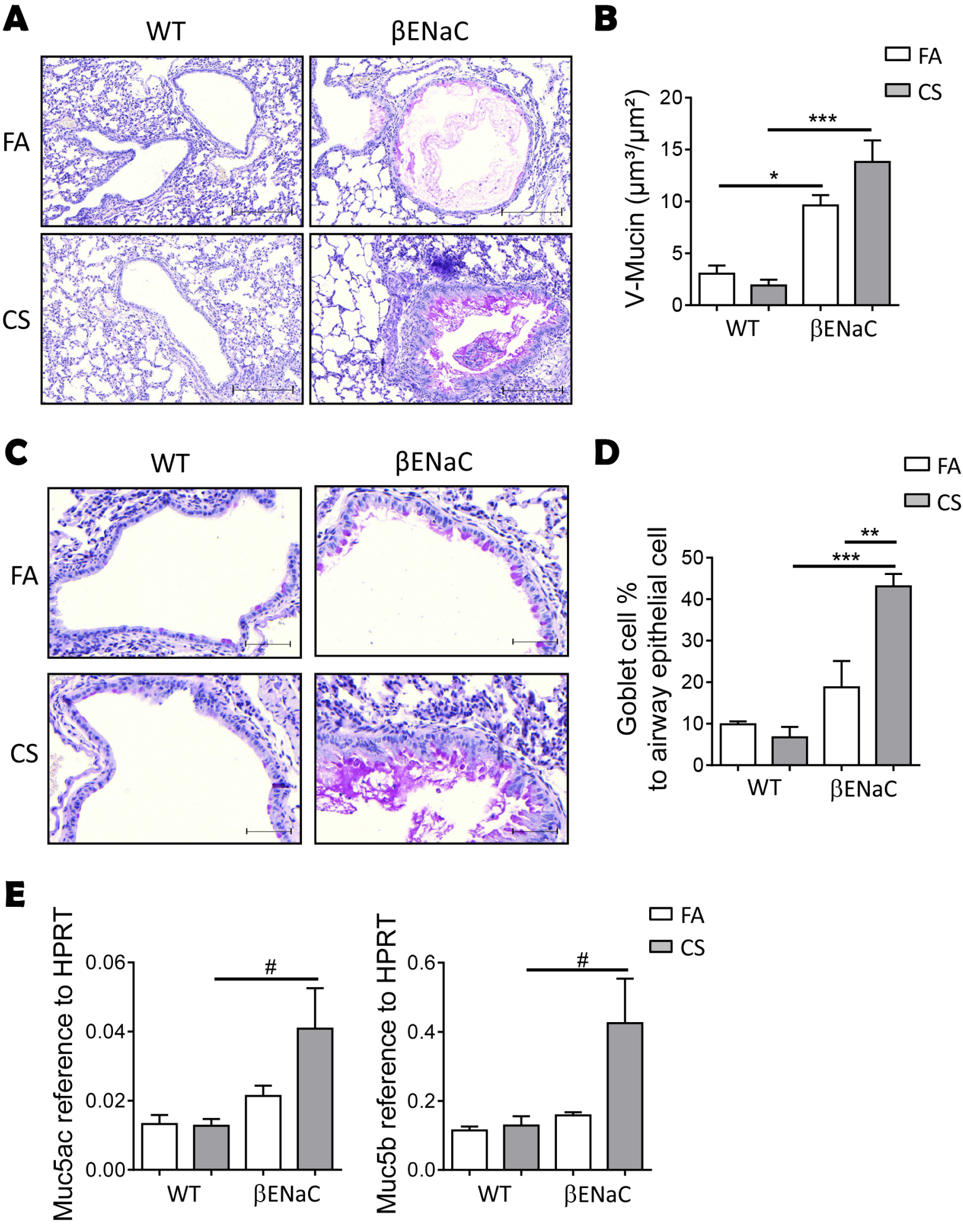
A
WT
βENaC
FA
CS
B
FA
CS
V-Mucin (μm³/μm²)
20
15
10
5
0
***
*
WT
βENaC
C
WT
βENaC
FA
CS
D
FA
CS
Goblet cell %
to airway epithelial cell
50
40
30
20
10
0
**
***
WT
βENaC
E
FA
CS
Muc5ac reference to HPRT
0.06
0.04
0.02
0.00
#
WT
βENaC
Muc5b reference to HPRT
0.6
0.4
0.2
0.0
#
WT
βENaC